Biosensors and Bioelectronics 132 (2019) 210–216

Contents lists available at ScienceDirect

Biosensors and Bioelectronics

journal homepage: www.elsevier.com/locate/bios

Backfilling rolling cycle amplification with enzyme-DNA conjugates on antibody for portable electrochemical immunoassay with glucometer readout

Lilin Ge[a,b,*,1], Bin Li[a,b,1], Houxi Xu[a], Wenyuan Pu[a], Hang Fai Kwok[b,*]

[a] State Key Laboratory Cultivation Base for TCM Quality and Efficacy, Nanjing University of Chinese Medicine, 138 Xianlin Avenue, Qixia District, Nanjing 210046, PR China

[b] Institute of Translational Medicine, Faculty of Health Sciences, University of Macau, Avenida de Universidade, Taipa, PR China

ARTICLE INFO

Keywords:
Electrochemical immunoassay
Rolling cycle amplification
Glucometer readout
Enzyme-DNA conjugates
Disease-related biomarker

ABSTRACT

A simple and feasible electrochemical immunosensing protocol with glucometer readout was designed for the detection of low-abundance disease-related biomarker (alpha-fetoprotein; AFP) on the basis of backfilling rolling cycle amplification (RCA) with invertase-DNA_2 conjugates on the detection antibody. The assay consisted of the immunoreaction, RCA reaction, DNA_2-invertase hybridization and glucose measurement. Initially, a sandwiched immunoreaction was carried out between anti-AFP capture antibody-coated microplate between nanogold-labeled pAb_2 detection antibody conjugated with DNA_1 primer (DNA_1-AuNP-pAb_2) in the presence of target ATP. Thereafter, the carried primers triggered the RCA reaction in the presence of circular DNA template, polymerase and dNTP, to produce numerous repeated oligonucleotide sequences for hybridization with many invertase-DNA_2 conjugates. The carried invertase molecules accompanying the hybridization reaction hydrolyzed sucrose into glucose, thereby resulting in the amplification of the detectable signal on a handheld personal glucometer (PGM). Under optimum conditions, the developed immunoassay exhibited high sensitivity for the quantitative screening of AFP within a dynamic range of 0.1–100 ng mL^{-1} at a low detection limit of 0.087 ng mL^{-1}. Other biomarkers and proteins did not interfere the signals of this system. In addition, this method was utilized to determine human serum samples containing target AFP, and received well-matched results with the referenced enzyme-linked immunosorbent assay (ELISA) method.

1. Introduction

Immunoassay, based on specific antigen-antibody reaction with high sensitivity, has gained increasing attention as a promising approach in analytical fields including environmental monitoring, food safety, and clinical diagnosis (Pei et al., 2013; Luo et al., 2018). Point-of-care testing (POCT; *i.e.*, bedside testing), defined as medical diagnostic testing at or near the point of care-that is, at the time and place of patient care, plays an important role on the development of advanced immunoassays thanks to its advantages of miniaturized devices and simple operation (Chinnadayyala et al., 2019; Quinn et al., 2016). This contrast with the historical patterns in which the testing was wholly or mostly confined to the medical laboratory, which entailed sending off specimens away from the point of care and then waiting hours or days to learn the results, during which time care must continue without the desired information (Guest et al., 2016). Recently, different POCT schemes have been reported and developed for the immunoassays coupling with portable personal glucometer, multimeter, pressure meter and smartphone (Tang et al., 2014; Qiu et al., 2017; Yu et al., 2019). Lai et al. (2017) developed a colorimetric immunoassay based on enzyme-controlled dissolution of MnO_2 nanoflakes with the enzyme cascade amplification. Yu et al. (2018) constructed a new enzyme immunoassay in a separate setup by coupling an aluminium-Prussian blue-based self-powered electrochromic display with the multimeter readout. Despite some advances in this field, there is still the requirement to explore innovative and powerful immunoassays with the aim of manufacturing portable and affordable diagnostic devices while preserving essential benefits in sensitivity, robustness and broad applicability.

Glucose meter, a medical device for determining the approximate concentration of glucose in the blood, can be a strip of glucose paper dipped into a substance and measured to the glucose chart (Hou et al.,

* Corresponding authors.
E-mail addresses: gelilin@njucm.edu.cn (L. Ge), hfkwok@um.edu.mo (H.F. Kwok).
[1] These authors have contributed equally to this work.

https://doi.org/10.1016/j.bios.2019.02.051
Received 16 January 2019; Received in revised form 17 February 2019; Accepted 21 February 2019
Available online 02 March 2019
0956-5663/

2014; Gao et al., 2014). Because of its portable size, easy operation, low cost and reliable quantitative results, personal glucose meter (PGM) has been become one of the most widely used devices in the world for the different applications, *e.g.*, to detect disease biomarkers, metal ions and small-molecular biotoxins (Chen and Yi, 2017; Li and Tang, 2017). Zhou and Tang (2018) utilized glucometer to determine arsenite on the basis of aptamer-graphene oxide-gated mesoporous silica nanocontainers. Ye et al. (2017) reported a sensitive sandwich immunoassay with a glucometer readout for portable and quantitative detection of Cronobacter sakazakii. For the successful development of PGM-based immunoassays, the signal amplification and noise reduction are crucial during the measurement, especially for the low-abundance biomolecules. Routine approaches are often used by coupling with enzyme labels because a single molecule of enzyme, *e.g.*, horseradish peroxidase, may cause the conversion of 10^7 molecules of substrate per minute (Zhang et al., 2013a; Lin et al., 2015). Unfavourably, one antibody can be usually conjugated covalently with only one enzyme molecule for steric reasons (Ren et al., 2018). In this regard, the sensitivity of the immunoassay based on the enzyme labels alone is always limited to some extent. To tackle this weakness, searching for new strategies by coupling with enzyme labels would be advantageous to obtaining low limits of detection and quantification.

Molecular biological technique, a branch of biology, concerns that molecular basis of biological activity between biomolecules in the various systems of a cell, including the interactions between DNA, RNA, proteins and their biosynthesis, as well as the regulation of the interactions (Lien and Lee, 2010). Significantly, recent researches have been focused on signal amplification with molecular biological methods, by employing DNA as the amplified indicators (Xiong et al., 2015; Zhou et al., 2018; Qiu et al., 2019; Zeng et al., 2019). Existing DNA-based amplification techniques mainly contain DNA-based thermal or isothermal cycling amplifications (Zhang et al., 2012). Rolling circle amplification (RCA) describes a process of unidirectional nucleic acid replication that can rapidly synthesize multiple copies of circular molecules of DNA/RNA with an isothermal enzymatic process (Zhang et al., 2013b, 2018a). As a simplified version of natural rolling circle replication, the RCA mechanism is widely used in molecular biology and biomedical nanotechnology, especially in the field of biosensing (as a method of signal amplification) (Zhang et al., 2018b). To this end, our motivation of this study is to combine the enzyme label and RCA product for the signal amplification of PGM-based immunoassay.

Alpha-fetoprotein (AFP) is a protein produced by the liver and yolk sac of a developing baby during pregnancy. Overexpression of the gene has been observed in acute liver injuries, indicating active liver regeneration (Wong et al., 2015). AFP has been associated with fatty liver disease, a disease that may lead to cirrhosis and hepatocellular carcinoma (Jacobson et al., 2014). It functions as a tumor marker for hepatocellular carcinoma. Herein we report on the proof-of-concept of powerful immunosensing platform for sensitive detection of AFP on personal glucometer by backfilling rolling cycle amplification (Scheme 1). The 'backfilling' process is carried out as follows: (i) the sandwiched immunoreaction is initially executed in the microplate by using nanogold-labeled DNA_1 primer and detection antibody; (ii) RCA reaction is then progressed accompanying formation of numerous DNA replicates in the presence of template and polymerase; and then (iii) the formed replicates on the replicates can hybridize/backfill with numerous invertase-DNA_2 conjugates to generate the enzymatic concatamers for the hydrolysis of sucrose molecules, thus resulting in the signal amplification.

2. Experimental

2.1. Chemicals and reagents

Monoclonal mouse anti-human AFP primary antibody (mAb_1; clone C3, purified from hybridoma cell culture; buffered aqueous solution; mol wt ~74 kDa; 1.0 mg mL^{-1}; immunohistochemistry: 2–4 μg mL^{-1}), polyclonal rabbit anti-human AFP antibody (pAb_2; buffered aqueous solution), human AFP ELISA kits including AFP standards, invertase from *Candida utilis* (Grade X, ≥300 units mg^{-1} solid; One unit will hydrolyze 1.0 μmole of sucrose to invert sugar per min at pH 4.5 at 55 °C), tris(2-carboxyethl)phosphine (TCEP), and sulfosuccinimidyl-4-(*N*-maleinidomethyl)-cyclohexane-1-carboxylat (sulfo-SMCC) were purchased from Merck KGaA (Darmstadt, Germany). T4 DNA ligase, deoxyribonucleoside 5′-triphosphates mixture (dNTP), adenosine 5′-triphosphate (ATP) and phi29 DNA polymerase were acquired from Takara Biotechnol. Co., Ltd. (Dalian, China). Sucrose and bovine serum albumin (BSA; Vetec™, reagent grade, ≥98%) were achieved from Aladdin (Shanghai, China). Gold nanoparticles (AuNPs; 250 nm in diameter, stabilized suspension in 0.1 mM PBS, reactant free) were purchased from Sigma-Aldrich LLC. (Shanghai, China) (note: The size with 250 nm in diameter was used as an example in this study). All other chemicals were of extra pure analytical grade and used without further purification. All the solutions were prepared with ultrapure water obtained from a Milli-Q water purifying system (≥18.2 MΩ cm, Milli-Q, Millipore). High-binding polystyrene 96-well microplates (Ref. 655061) were purchased from Greiner (Frickenhausen, Germany). A pH 9.6 carbonate coating buffer (1.59 g Na_2CO_3, 2.93 g $NaHCO_3$ and 0.2 g NaN_3) and a pH 7.4 phosphate-buffered saline (PBS, 10 mM) (2.9 g $Na_2HPO_4{\cdot}12H_2O$, 0.24 g KH_2PO_4, 0.2 g KCl and 8.0 g NaCl) were prepared by adding the corresponding chemicals into 1000-mL ultrapure water, respectively. The blocking buffer and washing buffer were obtained by adding 1.0 wt% BSA and 0.05% Tween 20 (v/v) in PBS, respectively.

All oligonucleotides used in the study were obtained from Sangon Biotech. Inc. (Shanghai, China). The sequences are listed as follows:

Thiol-DNA_1: 5′- HS-$(CH_2)_6$-CCG GTC GAA ATA GTG AGT-3′

Circular template: 5′-p-*TTC GAC CGG* AAC TGT CTT AGC AAA AAC TGT CTT AGC AA*A CTC ACT AT*-3′

Thiol-DNA_2: 5′-$(CH_2)_6$-CAC TAT TTC GAC-3′

The sequence at thiol-DNA_1 is the primer of RCA reaction. The italicized portion at the circular template (p = 5′ phosphate) matches the sequence of thiol-DNA_1, whereas the thiol-DNA_2 is the same as those in the italic on the circular template.

2.2. Preparation of DNA_1-AuNP-pAb_2

Nanogold-labeled DNA_1 primer with pAb_2 detection antibody (DNA_1-AuNP-pAb_2) was prepared similar to this work (Zhang et al., 2012). Prior to synthesis, gold colloids (5.0 mL, $C_{[Au]}$ = 24 μM) was initially adjusted to pH 9.0–9.5 using 0.1 M Na_2CO_3 aqueous solution. Thereafter, pAb_2 detection antibody (100 μL, 0.5 mg mL^{-1}) was added to gold nanoparticles, and incubated for 20 min at room temperature (rt). During this process, pAb_2 antibodies were covalently bound to gold nanoparticles *via* the dative binding between gold nanoparticles and free -SH groups of the antibody. Following that, the alkylthiol-capped barcode DNA_1 primer (300 μL, 0.5 OD) was injected into the mixture. After gently shaking for 5 min, the mixture was transferred to the refrigerator at 4 °C for further reaction (overnight). After that, the mixture was centrifuged (14,000 g) for 25 min at 4 °C. The pellet (*i.e.*, DNA_1-AuNP-pAb_2) was resuspended in sodium carbonate (1.0 mL, 2.0 mM) containing 1.0 wt% BSA and 0.1% sodium azide, pH 7.4, and stored at 4 °C until use. The as-prepared DNA_1-AuNP-pAb_2 conjugates were characterized by using high-resolution transmission electron microscopy (HRTEM; H-7650, Hitachi Instruments, Tokyo, Japan) and dynamic light scattering (DLS; Zetasizer Nano S90, Malvern, London, UK) (Please see Fig. S1 in the Supporting Information).

2.3. Preparation of DNA_2-invertase conjugates

The DNA_2-invertase conjugates were prepared resulting to previous works with minor modification (Xiang and Lu, 2011, 2012). Prior to

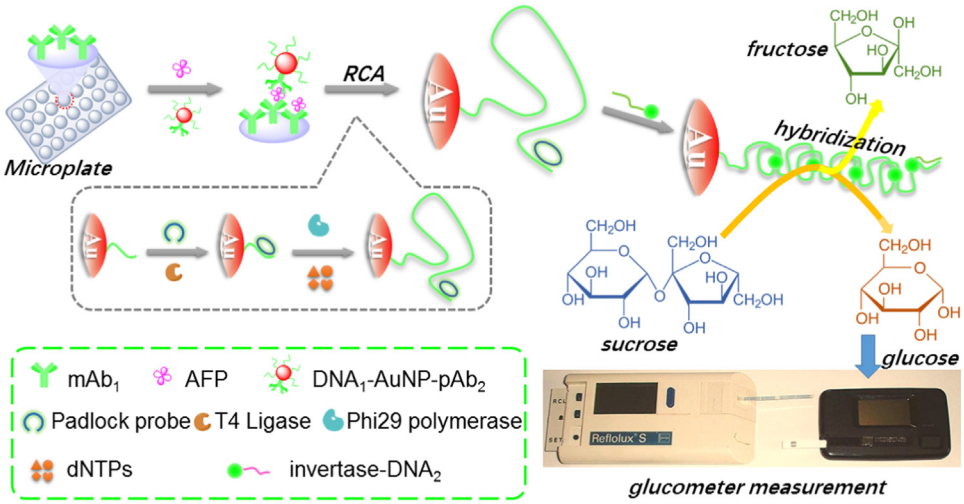

Scheme 1. Schematic illustration of rolling cycle amplification (RCA)-based electrochemical immunoassay for the detection of alpha-fetoprotein (AFP) on monoclonal mouse anti-human AFP antibody (mAb_1)-coated microplate with personal glucometer readout by using nanogold-labeled polyclonal anti-AFP detection and thiol-DNA_1 (DNA_1-AuNP-pAb_2), accompanying hybridization reaction of DNA_2-invertase with the RCA product.

synthesis, the thiolated DNA_2 strands were initially activated by mixing thiol-DNA_2 (30 μL, 1.0 mM) and TCEP (2.0 μL, 30 mM) aqueous solution with PBS (2.0 μL, 1.0 M, pH 5.5) in a centrifugal tube. After incubation for 60 min in the dark at rt, excess TCEP was removed by Amico Ultra-0.5 Centrifugal Filter Device (Amicon Ultra 100 K device, Billerica, MA) with PBS (10 mM, pH 7.4). Meanwhile, another solution was prepared by mixing sulfo-SMCC (1.0 mg) with invertase (400 μL, 20 mg mL^{-1}) in PBS (10 mM, pH 7.4), and then incubated for 60 min at rt under slight shaking on a shaker. Excess sulfo-SMCC was removed as before. Following that, TCEP-activated thiol-DNA_2 was rapidly added into sulfo-SMCC-activated invertase, and incubated overnight at rt with slight shaking on a shaker. Subsequently, the resulting mixture was purified by Amicon-100 K with PBS (10 mM, pH 7.4). Finally, the as-obtained product (*i.e.*, DNA_2-invertase) was dispersed into 1.0-mL PBS (10 mM, pH 7.4) and stored at 4 °C for further use.

2.4. Immunoreaction and PGM-based measurement

Scheme 1 gives the schematic illustration of backfilling rolling cycle amplification with enzyme-DNA_2 conjugates on antibody for portable electrochemical immunoassay for detection of AFP with glucometer readout. A high-binding polystyrene 96-well microplate (Ref. 655061, Greiner, Frickenhausen, Germany) was coated overnight at 4 °C with 50 μL per well of mAb_1 at a concentration of 10 μg mL^{-1} in 0.05 M sodium carbonate buffer (pH 9.6). The microplate was covered with adhesive plastic plate sealing film to prevent evaporation. On the following day, the plate was washed three time with washing buffer, and then incubated with 300 μL per well of blocking buffer for 60 min at 37 °C with shaking. The plate was then washed as before. Following that, 50 μL of AFP standards or samples with various concentrations and 50 μL of the above-prepared DNA_1-AuNP-pAb_2 suspension were simultaneously added into the microplate, and incubated for 60 min 37 °C under shaking. After washing again, 5.0 μL of circular template DNA (100 nM), 5.0 μL of T4 DNA ligase (4.0 U μL^{-1}), 90 μL of phi29 DNA polymerase (2 unit mL^{-1}) reaction buffer (50 mM, pH 7.5 Tris-HCl buffer, 10 mM magnesium acetate, 33 mM potassium acetate, 1.0 mM dithiothreitol, 10 mM dNTPs, and 0.1% Tween 20) and 1.0-mM ATP were added into the microplate, and incubated for 80 min at 37 °C to conduct the padlock ligation reaction and the RCA reaction. Subsequently, 100 μL of the above-prepared DNA_2-invertase conjugates was added to the microplate, and reacted for 60 min at 37 °C. The substrate sucrose (50 μL, 10 mM) was injected in the microplate, reacted for 10 min in PBS (10 mM, pH 4.5) at 55 °C (note: Use of pH 4.5 PBS and 55 °C was referred to the guideline of the invertase producer). Finally, a 3-μL aliquot of the supernatant was removed for glucose measurement by using the commercialized Roche PGM. The obtained signal was registered as the sensing signal relative to target AFP level. Note that the resulting microplate was washed with PBS (10 mM, pH 7.4) after each step. All measurements were carried out at room temperature (25 ± 1.0 °C). All data were obtained with three measurements each in parallel.

2.5. Monitoring of real samples with AFP ELISA kit

A commercialized enzyme immunoassay was utilized for the method comparison studies. For the sandwiched immunoassay with standard polystyrene 96-well plates, 50 μL of serum sample suspension was incubated at 37 °C for 60 min, and the wells were rinsed 3 times (3 min each) with 10 mM PBS (pH 7.4). Then we added 50-μL conjugate solution and incubation continued for 60 min. The wells were again rinsed and 50-μL 3,3′,5,5′-tetramethylbenzidine (TMB) reagent was added and incubated at 37 °C for 10 min. The enzymatic reaction was stopped by adding 50 μL of 2.0 M H_2SO_4 to each well. The results of ELISAs were measured using a spectrophotometric ELISA reader at a wavelength of 450 nm.

2.6. Statistical data analysis

A statistical data analysis was performed using Statistics Analysis System (SAS) ver. 9.0 and Statistical Program for Social Sciences (SPSS) ver. 9.0 software packages. Comparisons between the dependent variables were determined by using analysis of variance (ANOVA), Duncan multiple range test, correlation analysis and multiple regression analysis. Results are expressed as mean value ± standard deviation (SD) of three determinations and statistical significance was defined at $P \leq 0.05$.

All the experiments were performed in accordance with the Guidelines of Nanjing University of Chinese Medicine, and approved by the ethics committee at Nanjing University of Chinese Medicine, China. Informed consent was obtained for any experimentation with human subjects of this study.

3. Results and discussion

3.1. Design of RCA-based PGM immunoassay

In this work, mAb_1 capture antibody is initially immobilized onto the microplate *via* the physical adsorption of high-binding polystyrene microplate with the proteins, whilst the thiolated DNA_2 is covalently conjugated to the invertase by the interaction of TCEP-activated thiol-DNA_2 with sulfo-SMCC-activated invertase. The assay mainly consisted of the sandwich-type immunoreaction, RCA reaction and glucose

measurement. In the presence of target AFP, the sandwiched immunocomplex is formed between mAb_1-coated microplate and DNA_1-AuNP-pAb_2. Accompanying the immunocomplex, the carried DNA_1 on the DNA_1-AuNP-pAb_2 can be used as the primer to trigger the RCA reaction upon addition of circular DNA template, ligase and dNTPs. During this process, the short primer is extended under the catalysis of the polymerase to form a long single-stranded DNA by using the circular DNA template. Such a RCA product is a concatamer including numerous tandem repeats that are complementary to the circular template, which can be hybridized with the thiolated DNA_2 on the invertase, thereby resulting in the concatamer of numerous invertase molecules on the DNA strands. Upon the enzyme substrate glucose introduction, the concatenated invertase molecules catalyze the hydrolysis of glucose into glucose and fructose. The as-produced glucose molecules can be quantitatively determined on a portable personal glucometer with high sensitivity.

To construct such an RCA-based PGM immunosensing platform, one important precondition was whether the DNA_1 primer could induce the rolling cycle amplification in the polymerase and dNTPs. In this regard, gel electrophoresis was utilized to characterize the primer before and after reaction with the circular template and RCA (Fig. 1A). Lanes 1 and 2 represent the gel electrophoresis images of the unmodified DNA_1 and circular DNA template alone, respectively, which were in accordance with the natural base numbers of DNA_1 and circular template. When the primer reacted with the circular DNA template in the presence of polymerase and dNTPs, however, a long band was observed with different-number bases (lane 3). The reason was attributed to the fact that the primer in the solution could cause the formation of various-length RCA products. Such a long RCA product could provide a facilitation for the hybridization of DNA_2-invertase conjugates.

3.2. Activity detection of the labeled invertase on the thiolated DNA_2

As mentioned above, DNA_2-invertase conjugates were prepared *via* the covalent binding between the invertase protein and the thiol-DNA_2. Commonly, one major problem associated with the covalent binding is the decrease of enzymatic activity when the proteins are exposed to the reactive groups and the harsh reaction conditions. To investigate the enzymatic activity of invertase after conjugation with the thiolated DNA_2, sucrose standards with different concentrations were initially injected into the above-prepared DNA_2-invertase (50 μL) mixture, and then incubated for 10 min in PBS (10 mM, pH 4.5) at 55 °C. The resulting products were determined on the portable PGM, respectively. As shown in Fig. 1B, the labeled invertase on the DNA_2-invertase followed a classical Michaelis-Menten behaviour in PBS (10 mM, pH 4.5), indicating that the conjugated invertase with the DNA_2 could exhibit the significant catalytic responses due to the hydrolysis of the substrate sucrose. Thus, the as-prepared DNA_2-invertase conjugates could be preliminarily employed for PGM-based detection method.

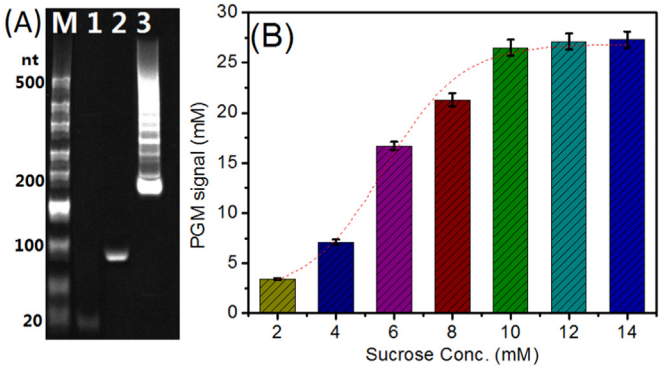

Fig. 1. (A) Gel electrophoresis (M: marker; lane 1: DNA_1; lane 2: circular DNA template; and lane 3: RCA product); and (B) activity measurement of DNA_2-invertase (50 μL) with different-concentration sucroses.

3.3. Control tests and feasibility evaluation

To monitor the feasibility of this method during the measurement, DNA_1-AuNP-pAb_2 and DNA_2-invertase were used for the detection of target AFP in mAb_1-coated microplate by coupling with primer-triggered RCA reaction. Firstly, the immunoassay processes after each step were investigated in the presence of sucrose in order to demonstrate whether the as-produced glucose derived from the final invertase toward the hydrolysis of sucrose. Note that the products after each step reacted with circular DNA template, ligase, polymerase, dNTPs, DNA_2-invertase and sucrose, respectively, as described in the Experimental section. As seen from columns '*a*-*b*' in Fig. 2A, almost no PGM signals were achieved at mAb_1-coated microplate before and after reaction with target AFP (10 ng mL^{-1} used in this case), respectively. Upon the DNA_1-AuNP-pAb_2 introduction, significantly, a strong PGM signal was acquired (column '*c*') after the immunocomplex formation. To verify that DNA_1-AuNP-pAb_2 could be conjugated to mAb_1-coated microplate in the presence of target AFP, we also utilized scanning electron microscopy (SEM; Hitachi S4800, Japan) to characterize the interfaces (Fig. S2 in the Supporting Information). Relative to AFP/mAb_1-coated microplate (Fig. S2-A), DNA_1-AuNP-pAb_2 could be clearly observed by the antigen-antibody reaction (Fig. S2-B). Logically, one question arises as to whether the detectable PGM signal originated from the non-specific adsorption of the mAb_1-coated microplate toward DNA_2-invertase. To clarify this concern, DNA_2-invertase conjugates were directly added into the mAb_1-coated microplate in the absence of target AFP. Following that, the circular DNA template, ligase, polymerase and dNTPs were injected in this system. The resulting product was incubated with sucrose. Inspiringly, the PGM signal was almost the same as that of mAb_1-coated microplate (column '*d*' *vs.* column '*a*'). The results further revealed that the strong PGM signal stemmed from the specific antigen-antibody reaction and the RCA reaction, accompanying the hydrolysis of sucrose.

Certainly, another question to be answered was whether the PGM signal derived from the hydrolysis of sucrose through the invertase. In this case, we also used cyclic voltammetry to measure the product. Initially, glucose oxidase (GOx) was immobilized on a cleaned glassy carbon electrode by using the acidic chitosan solution. Thereafter, the resulting electrode was monitored in PBS (10 mM, pH 7.4) containing 10 mM $Fe(CN)_6^{4-/3-}$ at 50 mV s^{-1} (Fig. 2B). The resulting products in the presence (column '*c*') and absence (column '*d*') of target AFP in Fig. 2A were added into the solution, respectively. Curve '*a*' gives the cyclic voltammogram of GOx-modified electrode. Upon addition of the product of column '*c*' in Fig. 2A, the anodic peak current increased, whereas the cathodic peak current decreased (Fig. 2B, curve '*b*'). When the product of column '*c*' in Fig. 2A, however, the cyclic voltammogram was almost the same as that of curve '*a*'. The results indicated that glucose molecules could be produced in the presence of target AFP by the hybridized DNA_2-invertase.

3.4. Optimization of experimental conditions

As described above, the amplification of PGM-based immunosensing signal mainly originated from the RCA product. Typically, the amount of the product directly depended on the RCA reaction time. As shown in Fig. S3-A in the Supporting Information, the PGM signal increased with the increasing RCA reaction time, and tended to level off after 80 min. A longer reaction time did not cause the significant increase in the signal. To save the assay time, 80 min was selected for RCA reaction.

Accompanying formation of the long RCA single-stranded DNA, the hybridization of DNA_2-invertase with the product was also very crucial for the hydrolysis of sucrose. Fig. S3-B displays the dependence of PGM signal of the electrochemical immunoassay on hybridization time with DNA_2-invertase. A maximum PGM signal could be achieved after

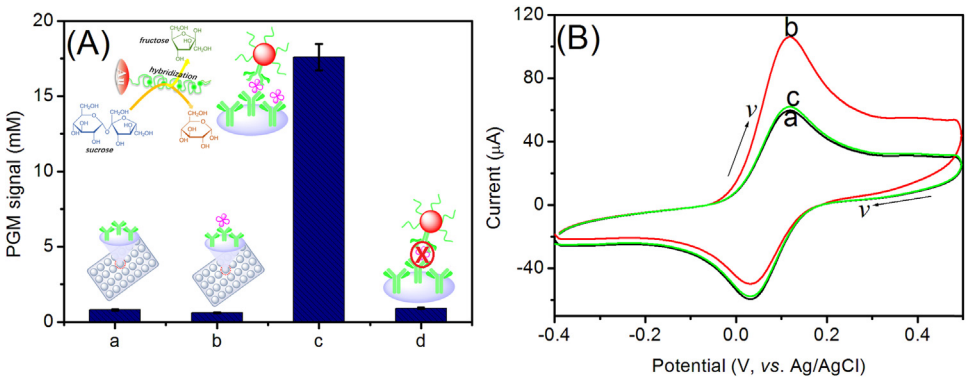

Fig. 2. (A) PGM responses of (*a*) mAb_1-coated microplate, (*b*) substrate '*a*' + 10 ng mL^{-1} AFP, (*c*) substrate '*b*' + DNA_1-pAb_2 and (*d*) substrate '*a*' + DNA_1-pAb_2 (note: The substrate reacted with RCA and DNA_2-invertase after each step in the presence of sucrose); (B) cyclic voltammograms of (*a*) GOx-modified glassy carbon electrode, (b) electrode '*a*' + the product after reaction of mAb_1-coated microplate with 10 ng mL^{-1} AFP and DNA_1-pAb_2, and (c) electrode '*a*' + the product after reaction of mAb_1-coated microplate with DNA_1-pAb_2 in the absence of target AFP in PBS (10 mM, pH 7.4) containing 10 mM $Fe(CN)_6^{4-/3-}$ at 50 mV s^{-1}.

60 min. To ensure the adequate reaction with DNA_2-invertase, 60 min was utilized for the hybridization of RCA product with the DNA_2-invertase conjugates.

3.5. Analytical performance of PGM-based immunoassay toward AFP

Under optimal conditions, the sensitivity and calibration plots of the PGM-based immunoassay were studied for target AFP with different concentrations, by using RCA for the signal amplification. The final product through the hydrolytic reaction of invertase toward sucrose was determined on a portable glucometer. As shown Fig. 3A, the PGM signal displayed a typical sigmoidal '*S*' response relationship with the logarithm of AFP concentrations. A good linear dependence between PGM signal and AFP level could be achieved within the range of 0.1–100 ng mL^{-1}. The linear regression equation was fitted to $y = (8.91 \pm 0.56) \times \log C_{[AFP]}$ (ng mL^{-1}) + (8.95 ± 0.62) with a correlation coefficient (*r*) of 0.9904 (*n* = 7). The limit of detection (LOD) was calculated to 87 pg mL^{-1} AFP at a signal-to-noise ratio of 3. To further embody the advantages, the analytical properties of this system including the linear range and LOD were compared with other

Table 1
Comparison of analytical properties of PGM-based immunoassay with other portable detection schemes for target AFP.

Detection device	Linear range (ng mL^{-1})	LOD (pg mL^{-1})	Refs.
Luminometer	0.05–1000	16	Liu et al. (2018)
Potentiometry	0. –100	68	Li et al. (2018)
Lateral flow device	1.0–100	1000	Preechakasedkit et al. (2018)
Pressure gauges	10–200	3400	Wang et al. (2017)
Portable UV–vis spectrometer	1.0–1000	1000	Kim et al. (2017)
Glucometer	0.1–50	30	Wu et al. (2015)
Glucometer	–	180	Zhu et al. (2014)
Glucometer	0.1–100	87	This work

AFP detection schemes (Table 1). As indicated from Table 1, the LOD of PGM-based immunoassay was partially lower than those of other portable detection devices. The reason might be attributed to the facts that (i) the formed long single-stranded DNA by RCA reaction hindered the

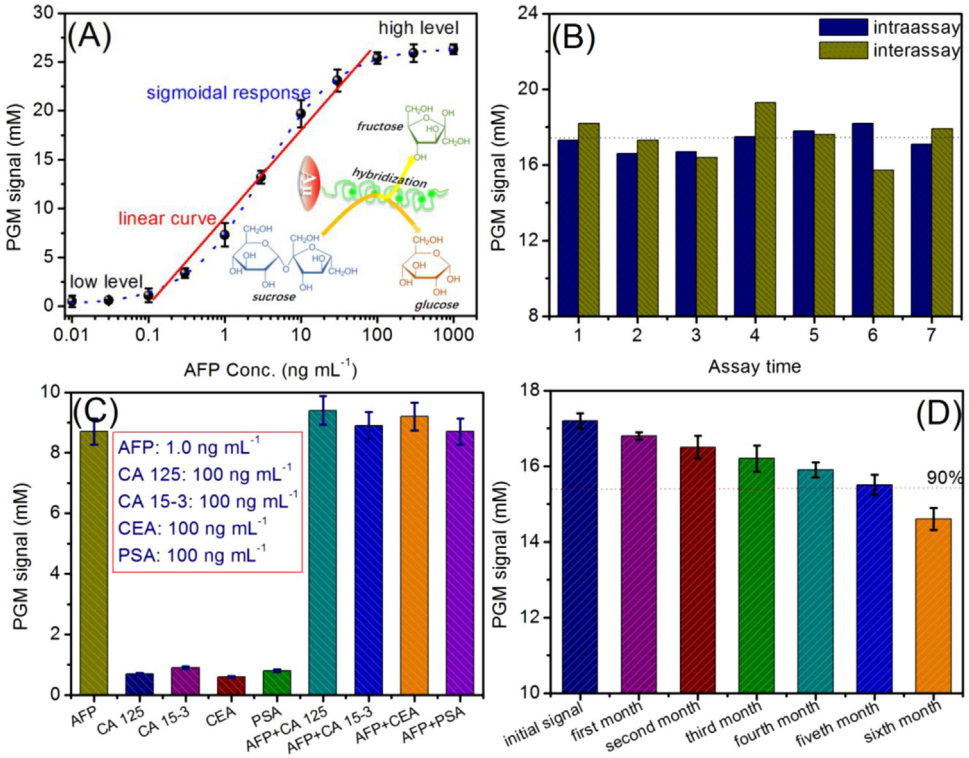

Fig. 3. (A) PGM responses of RCA-based immunoassay for AFP standards with different concentrations; and the (B) precision, (C) specificity and (D) storage stability of DNA_1-AuNP-pAb_2 and DNA_2-invertase-based immunoassay. Error bars represent the standard deviation (*n* = 3).

Table 2
Accuracy evaluation for human serum samples between PGM-based immunosensing method and commercial human AFP ELISA kit.

Sample no.	Method (mean ± SD, ng mL^{-1}; n = 3)[a]		t_{exp}
	PGM immunoassay	ELISA kit	
1	56.7 ± 5.6	54.1 ± 3.1	0.71
2	89.3 ± 5.2	93.4 ± 4.6	1.02
3	34.5 ± 1.1	30.2 ± 1.4	4.18
4	13.2 ± 0.5	11.6 ± 0.8	2.94
5	1.41 ± 0.11	1.58 ± 0.07	2.26
6	0.12 ± 0.01	0.13 ± 0.01	1.23

[a] Samples 5–6 were obtained by diluting sample 4 to 10-fold and 100-fold, respectively.

hybridization of invertase-DNA_2 conjugates to some extent because of the steric hindrance effect, and (ii) the hydrolytic efficiency of invertase was lower than that of oxidoreductase activity [*e.g.*, A single molecule of horseradish peroxidase may cause the conversion of 10^7 molecules of substrate per minute (Zhang et al., 2013a)] since pH and temperature heavily affected the activity of hydrolases. Compared with commerial AFP ELISA kits, the proposed method looks much more complicated. However, our stategy did not need the expensive instruments. Furthermore, another advantage of our strategy depended on the fact that PGM-based immunoassay combined with the nanolabel, enzyme label and molecular biological amplification technique for the glucometer readout with the signal amplification.

3.6. Reproducibility, selectivity and stability

The precision of RCA-based PGM electrochemical immunoassay was evaluated for the detection of 10 ng mL^{-1} AFP using the as-prepared DNA_1-AuNP-pAb_2 and DNA_2-invertase at the different batches. The results indicated that the relative standard deviations (RSDs) were 3.3% and 6.8% (n = 7) for the intra-assay and inter-assay, respectively (Fig. 3B). Although the RSD for the inter-assay was more than that of the intra-assay, the reproducibility of RCA-based PGM immunoassay was acceptable.

Next, we also investigated the selectivity of the RCA-based PGM electrochemical immunoassay against the non-targets, *e.g.*, cancer antigen 125 (CA 125), cancer antigen 15-3, carcinoembryonic antigen (CEA) and prostate-specific antigen (PSA). As shown in Fig. 3C, the PGM signals of the immunoassay were almost close to zero toward these non-targets. In contrast, the strong PGM signals were obtained in the presence of only target AFP. Hence, RCA-based immunoassay had good specificity toward target AFP.

Further, the storage stability of the as-prepared DNA_1-AuNP-pAb_2 and DNA_2-invertase was measured during a six-month storage period. They were stored at 4 °C when not in use. By using 10 ng mL^{-1} AFP as an example, the PGM signals could preserve 90% of the initial signal after storage them for five months, respectively (Fig. 3D), suggesting a good stability.

3.7. Analysis of human serum specimens

The accuracy of RCA-based PGM electrochemical immunoassay was evaluated by assaying human serum specimens, and compared with the commercial human AFP ELISA kit. These serum specimens were obtained from our hospital according to the rules of the local ethical committee. During the measurements, all handing and processing were performed carefully, and all the tools in contact with patient specimens were disinfected after use. Moreover, informed consent was obtained from any experimentation with human subjects. The amount of AFP concentration in these samples were calculated by the above-mentioned regression equation during the measurement. All the results obtained from these two methods are listed in Table 2. Evaluation of the accuracy between two methods was executed by using a classical t-test. Clearly, all the t_{exp} values in all cases were below t_{crit} ($t_{crit[2,\ 0.05]}$ = 4.30), indicating well-matched results between two methods. Hence, RCA-based PGM electrochemical immunoassay could be preliminarily applied for the detection of AFP in the complex samples.

4. Conclusions

In summary, this work designs an *in-situ* signal-amplified glucometer-based electrochemical immunoassay for the quantitative screening of disease-related biomarker, AFP, by coupling high-efficient enzyme labelling strategy with molecular biological amplification technique. The sandwiched immunoreaction was carried out in the low-cost microplate, whereas the signal was amplified through rolling cycle amplification reaction. The backfilling DNA_2-invertase conjugates on the RCA product caused the generation of PGM signal in the presence of the substrate sucrose. Experimental results indicated that the developed immunoassay exhibited high sensitivity, good specificity and acceptable method accuracy for analysis of real samples without the need of expensive instrumentations. Nevertheless, one major disadvantage of our system involves in the long incubation time for RCA reaction and DNA hybridization. Therefore, future work should focus on improvement of the molecular biological technique during the incubation process.

Acknowledgment

This work is supported by the National Natural Science Foundation of China (Grant no.: 81703750) and the MOST-FDCT joint project between the International S&T Cooperation Program of China (Grant no.: 2016YFE0121900) & the Science and Technology Development Fund of Macau SAR (Grant no.: FDCT 023/2015/AMJ). The authors would like to thank Prof. Renxiang Tan for his constructive comments and suggestions on this study.

Declaration of interests

None.

Credit author statement

Lilin Ge and Hang Fai Kwok designed the study. Lilin Ge and Bin Lin performed major part of this research including experiment, analysis and interpretation of data. Houxi Xu and Wenyuan Pu helped to search literatures and to draw figures. Lilin Ge and Hang Fai Kwok supervised the whole project and wrote the manuscript. The authors agree to be accountable for all aspects of the work. The final version has been approved by all authors.

Appendix A. Supporting information

Supplementary data associated with this article can be found in the online version at https://doi.org/10.1016/j.bios.2019.02.051.

References

Chen, Y., Yi, H., 2017. Anal. Methods 9, 2933–2938.
Chinnadayyala, S., Park, J., Le, H., Santhosh, M., Kadam, A., Cho, S., 2019. Biosens. Bioelectron. 126, 68–81.
Gao, Z., Tang, D., Xu, M., Chen, G., Yang, H., 2014. Chem. Commun. 50, 6256–6258.
Guest, F., Guest, P., Martins-De-Souza, D., 2016. Biomark. Med. 10, 431–443.
Hou, L., Zhu, C., Wu, X., Chen, G., Tang, D., 2014. Chem. Commun. 50, 1441–1443.
Jacobson, H., Bersen, T., Bennett, J., 2014. Cancer Prev. Res. 7, 565–573.
Kim, D., Kim, J., Kwak, C., Heo, N., Oh, S., Lee, H., Lee, G., Vilian, A., Han, Y., Kim, W., Kim, G., Kwon, S., Huh, Y., 2017. J. Cryst. Growth 469, 131–135.
Lai, W., Wei, Q., Xu, M., Zhuang, J., Tang, D., 2017. Biosens. Bioelectron. 89, 645–651.
Li, G., Tang, D., 2017. J. Mater. Chem. B 5, 5573–5579.

Li, Q., Jin, J., Lou, F., Tang, D., 2018. Sci. Chin. Chem. 61, 750–756.
Lien, K., Lee, G., 2010. Analyst 135, 1499–1518.
Lin, Y., Zhou, Q., Lin, Y., Tang, D., Niessner, R., Knopp, D., 2015. Anal. Chem. 87, 8531–8540.
Liu, P., Fang, X., Cao, H., Gu, M., Kong, J., Deng, A., 2018. Anal. Chim. Acta 1039, 98–107.
Luo, Z., Zhang, L., Zeng, R., Su, L., Tang, D., 2018. Anal. Chem. 90, 9568–9575.
Pei, X., Zhang, B., Tang, J., Liu, B., Lai, W., Tang, D., 2013. Anal. Chim. Acta 758, 1–18.
Preechakasedkit, P., Siangproh, W., Khongchareonporn, N., Ngamrojanavanich, N., Chailapakul, O., 2018. Biosens. Bioelectron. 102, 27–32.
Qiu, Z., Shu, J., Tang, D., 2017. Anal. Chem. 89, 5152–5160.
Qiu, Z., Shu, J., Liu, J., Tang, D., 2019. Anal. Chem. 91, 1260–1268.
Quinn, A., Dixon, D., Meenan, B., 2016. Crit. Rev. Clin. Lab Sci. 53, 1–12.
Ren, R., Cai, G., Yu, Z., Tang, D., 2018. Sens. Actuator B 265, 174–181.
Tang, D., Lin, Y., Zhou, Q., Lin, Y., Li, P., Niessner, R., Knopp, D., 2014. Anal. Chem. 86, 11451–11458.
Wang, Q., Li, R., Shao, K., Lin, Y., Yang, W., Guo, L., Qiu, B., Lin, Z., Chen, G., 2017. Sci. Rep. 7 (art. no. 45343).
Wong, R., Ahmed, A., Gish, R., 2015. Clin. Liver Dis. 19, 309–323.
Wu, S., Chen, J., Tian, Y., Tang, X., Li, W., Li, J., 2015. Anal. Methods 7, 1843–1848.
Xiong, E., Zhang, X., Liu, Y., Zhou, J., Yu, P., Li, X., Chen, J., 2015. Anal. Chem. 87, 7291–7296.
Xiang, Y., Lu, Y., 2011. Nat. Chem. 3, 697–703.
Xiang, Y., Lu, Y., 2012. Anal. Chem. 84, 1975–1980.
Ye, L., Zhao, G., Dou, W., 2017. Anal. Methods 9, 6286–6291.
Yu, Z., Cai, G., Ren, R., Tang, D., 2018. Analyst 143, 2992–2996.
Yu, Z., Tang, Y., Cai, G., Ren, R., Tang, D., 2019. Anal. Chem. 91, 1222–1226.
Zeng, R., Luo, Z., Su, L., Zhang, L., Tang, D., Niessner, R., Knopp, D., 2019. Anal. Chem. 91, 2447–2454.
Zhang, B., Liu, B., Tang, D., Niessner, R., Chen, G., Knopp, D., 2012. Anal. Chem. 84, 5392–5399.
Zhang, B., Tang, D., Goryacheva, I., Niessner, R., Knopp, D., 2013a. Chem. Eur. J. 19, 2496–2503.
Zhang, B., Liu, B., Zhou, J., Tang, J., Tang, D., 2013b. ACS Appl. Mater. Interfaces 5, 4479–4485.
Zhang, K., Lv, S., Lin, Z., Li, M., Tang, D., 2018a. Biosens. Bioelectron. 101, 159–166.
Zhang, K., Lv, S., Lu, M., Tang, D., 2018b. Biosens. Bioelectron. 117, 590–596.
Zhou, Q., Tang, D., 2018a. J. Mater. Chem. B 6, 6585–6591.
Zhou, Q., Lin, Y., Zhang, K., Li, M., Tang, D., 2018b. Biosens. Bioelectron. 101, 146–152.
Zhu, X., Zheng, H., Xu, H., Lin, R., Han, Y., Han, Y., Yang, G., Lin, Z., Guo, L., Qiu, B., Chen, G., 2014. Anal. Methods 6, 5264–5268.